BIOMOLECULES & THERAPEUTICS

Original Article
Biomol Ther 28(5), 473-481 (2020)

Synergistic Induction of Apoptosis by the Combination of an Axl Inhibitor and Auranofin in Human Breast Cancer Cells

Yeon-Sang Ryu†, Sangyun Shin†, Hong-Gyu An, Tae-Uk Kwon, Hyoung-Seok Baek, Yeo-Jung Kwon and Young-Jin Chun*

Center for Metareceptome Research, College of Pharmacy, Chung-Ang University, Seoul 06974, Republic of Korea

Abstract

Axl receptor tyrosine kinase has been implicated in cancer progression, invasion, and metastasis in various cancer types. Axl overexpression has been observed in many cancers, and selective inhibitors of Axl, including R428, may be promising therapeutic agents for several human cancers, such as breast, lung, and pancreatic cancers. Here, we examined the cell growth inhibition mediated by R428 and auranofin individually as well as in combination in the human breast cancer cell lines MCF-7 and MDA-MB-231 to identify new advanced combination treatments for human breast cancer. Our data showed that combination therapy with R428 and auranofin markedly inhibited cancer cell proliferation. Isobologram analyses of these cells indicated a clear synergism between R428 and auranofin with a combination index value of 0.73. The combination treatment promoted apoptosis as indicated by caspase 3 activation and poly (ADP-ribose) polymerase cleavage. Cancer cell migration was also significantly inhibited by this combination treatment. Moreover, we found that combination therapy significantly increased the expression level of Bax, a mitochondrial proapoptotic factor, but decreased that of the X-linked inhibitor of apoptosis protein. Furthermore, the suppression of cell viability and induction of Bax expression by the combination treatment were recovered by treatment with N-acetylcysteine. In conclusion, our data demonstrated that combined treatment with R428 and auranofin synergistically induced apoptosis in human breast cancer cells and may thus serve as a novel and valuable approach for cancer therapy.

Key Words: Axl receptor tyrosine kinase, Auranofin, Bax, Synergism

INTRODUCTION

Breast cancer is the most common cancer among woman and the leading cause of cancer-related death in females worldwide (Nagini, 2017). Over past several decades, the mortality rate of patients with breast cancer has declined substantially owing to regular cancer screening and the application of various therapies, such as radiotherapy, chemotherapy, and surgery (Jin and Ye, 2013). Among the breast cancer subtypes, triple-negative breast cancers (TNBCs) lacking the estrogen receptor (ER), the progesterone receptor (PR), and human epidermal growth factor receptor 2 (HER2) account for 15-20% of all breast cancers and are more aggressive than other forms of breast cancer; moreover, they show a high degree of proliferation and metastasis (Yao *et al*., 2017; Jung, 2019). Since TNBC cells lack hormone receptors, classical therapies targeting ER, PR, and HER2 may be ineffective. Therefore, TNBC is more difficult to cure than the other subtypes (Gelmon *et al*., 2012; Vidula and Bardia, 2017). Hence, finding new drug targets and advanced treatment methods is crucial.

Axl is a surface receptor located on the cell surface; it transduces extracellular signals into the cytosol via binding growth factors (Miller *et al*., 2016). Recently, the relationship between Axl and cancer was revealed. Axl overexpression has been shown to be associated with tumor progression as well as cancer cell migration that predicts aggressive behavior (Holland *et al*., 2010). Furthermore, Axl activation was found to be correlated with a poor survival rate in breast cancer, especially TNBC (Zhang *et al*., 2008; Leconet *et al*., 2017). Axl receptor tyrosine kinase has emerged as an important mediator of drug-resistance and immune escape in TNBC, and recent studies have demonstrated that the Gas6/Axl axis may represent a therapeutic target for chemoresistance and metastasis in breast cancer (Wang *et al*., 2016). However, the precise mechanism of Axl in cancer remains unclear.

Open Access **https://doi.org/10.4062/biomolther.2020.051**

Received Apr 3, 2020 **Revised** May 14, 2020 **Accepted** Jun 1, 2020
Published Online Jun 15, 2020

***Corresponding Author**
E-mail: yjchun@cau.ac.kr
Tel: +82-2-820-5616, Fax: +82-2-825-5616
†The first two authors contributed equally to this study.

R428 (BGB324, bemcentinib) is an anticancer drug candidate under clinical investigation. R428 is known to bind to the catalytic kinase domain of Axl and suppress kinase activity (Gay *et al*., 2017). It is a selective Axl inhibitor with an IC_{50} of 14 nM and has more than 50-fold sensitivity for Axl than for Abl, Mer, Tyro3, InsR, EGFR, HER2, and PDGFR. R428 has been shown to inhibit the receptor tyrosine kinase Axl, leading to cell death in many types of cancers. In addition, R428 was shown to act synergistically with cisplatin to promote the inhibition of liver metastasis (Holland *et al*., 2010).

Auranofin is a gold phosphine derivative used in the treatment of rheumatoid arthritis (Shaw, 1999). Additionally, it is also an effective anticancer agent (Varghese and Busselberg, 2014). Auranofin is a thioredoxin reductase inhibitor and is currently under clinical trials for chronic lymphocytic leukemia (Fiskus *et al*., 2014). Previous studies demonstrated that auranofin exerts cytotoxic activity by increasing the production of reactive oxygen species (ROS) (Oommen *et al*., 2016). According to our previous study, the inhibition of PI3K/Akt signaling by the combination of auranofin and Mesupron might be a potential mechanism underlying their synergistic induction of apoptosis in human breast cancer cells (Lee *et al*., 2017).

R428, trastuzumab, and lapatinib, when used in combination, have been shown to synergistically inhibit metastasis in HER2+ breast cancer cells (Goyette *et al*., 2018). Thus, in the present study, the effects of the combination of R428 and auranofin on TNBC cells (MDA-MB-231) as well as $HER2^+$ breast cancer cells (MCF-7) were determined.

MATERIALS AND METHODS

Chemicals and reagents

Auranofin, N-acetylcysteine (NAC), and mitomycin C were purchased from Sigma-Aldrich (St. Louis, MO, USA). R428 was purchased from Selleckchem (Houston, TX, USA). RPMI 1640 medium and fetal bovine serum (FBS) were obtained from HyClone (Logan, UT, USA). The bicinchoninic acid (BCA) protein assay kit and enhanced chemiluminescence (ECL) kit were purchased from Thermo Fisher Scientific (Waltham, MA, USA). The EZ-CyTox cell viability assay kit was obtained from Daeil Lab Service (Seoul, Korea). The ECL kit was obtained from Bionote (Gyeonggi, Korea). UltraCruz™ Mounting Medium and Texas Red-conjugated goat anti-rabbit IgG were purchased from Santa Cruz Biotechnology (Santa Cruz, CA, USA). M-MLV reverse transcriptase and RNase inhibitor were purchased from Promega (Madison, WI, USA). Ex Taq polymerase was purchased from TaKaRa Bio (Shiga, Japan). SYBR green was purchased from Qiagen (Hilden, Germany). Rabbit polyclonal antibody for Bax was purchased from Santa Cruz Biotechnology, and rabbit polyclonal antibody for poly (ADP-ribose) polymerase (PARP) was purchased from Cell Signaling Technology (Beverly, MA, USA). All other chemicals and reagents were of the highest quality commercially available.

Cell culture

MDA-MB-231, MCF-7, Hep3B, PC-3, HeLa, and H520 cells were obtained from Korea Cell Line Bank (KCLB, Seoul, Korea). The cells were cultured in RPMI 1640 medium supplemented with 10% (v/v) heat inactivated FBS, 100 U/mL penicillin, and 100 μg/mL streptomycin and maintained at 37°C in a humidified atmosphere of 5% CO_2.

Cell viability assay

The cells (0.7×10^4 cells/well) were plated in 96-well plates and incubated at 37°C for 24 h. Then, the cells were treated with varying concentrations of R428 and auranofin for 48 h. Next, 10 μL of EZ-CyTox solution was added and the cells were incubated for 60 min at 37°C. The produced formazan dyes were quantified by measuring the absorbance at 450 nm using the Sunrise™ microplate reader (Tecan, Männedorf, Switzerland). All experiments were independently performed at least three times.

Transient transfection with siRNA

Specific siRNAs for Axl or thioredoxin reductase (Qiagen) were used in the transfection experiments. The cells were transfected with 40 nM siRNA using a transfection system (Invitrogen, Carlsbad, CA, USA) and cultured in 60-mm dishes in RPMI 1640 medium containing 10% FBS without antibiotics for 24 h at 37°C in a humidified 5% CO_2 atmosphere. Subsequently, the cells were maintained in RPMI 1640 medium containing 10% FBS for 48 h.

Western blotting

The cells were harvested by scraping and solubilized in ice-cold lysis buffer containing 50 mM Tris-HCl (pH 8.0), 1% NP-40, 150 mM NaCl, 0.5% sodium deoxycholate, 2 mM EDTA, 0.1% sodium dodecyl sulfate (SDS), and 50 mM NaF. Protein concentration was determined using the BCA Protein Assay Reagent. Extracted proteins (20-40 μg) were resolved on 8-15% SDS-polyacrylamide gels and electrochemically transferred onto PVDF membranes. The membranes were then blocked with skim milk (5%) or bovine serum albumin (BSA; 5%, w/v) in Tris-buffered saline for 4 h at 4°C and incubated overnight with specific primary antibodies (1:1,000 dilution). Subsequently, the membranes were washed with phosphate-buffered saline (PBS) and incubated with secondary antibodies (1:5,000 dilution) for 3 h at 4°C. Protein bands were then visualized by ECL and assessed using the ChemiDox XRS densitometer (Bio-Rad, CA, USA). Quantitative data were analyzed using Quantity One software (Bio-Rad).

Confocal microscopy

The cells were treated with the chemicals for the indicated durations of time and cultured on poly D-lysine-coated coverslips. After 48 h, the cells were washed with PBS at least three times and fixed with 3.7% paraformaldehyde in PBS for 10 min at room temperature. After washing with PBS, the fixed cells were permeabilized with 0.5% Triton X-100 for 15 min and then washed again with PBS several times. After blocking with 3% BSA in cold PBS at room temperature for 60 min, the cells were incubated overnight with primary antibody (1:200) (Santa Cruz) at 4°C. The cells were then washed with PBS three times for 3 min and incubated with goat anti-rabbit IgG-Texas Red (1:200) for 6 h at room temperature. After additional washes with cold PBS, the coverslips were mounted on glass slides using UltraCruz™ Mounting Medium (Santa Cruz). Fluorescence signals were analyzed using the Zeiss LSM 800 confocal laser scanning microscope (Carl-Zeiss, Oberkochen, Germany).

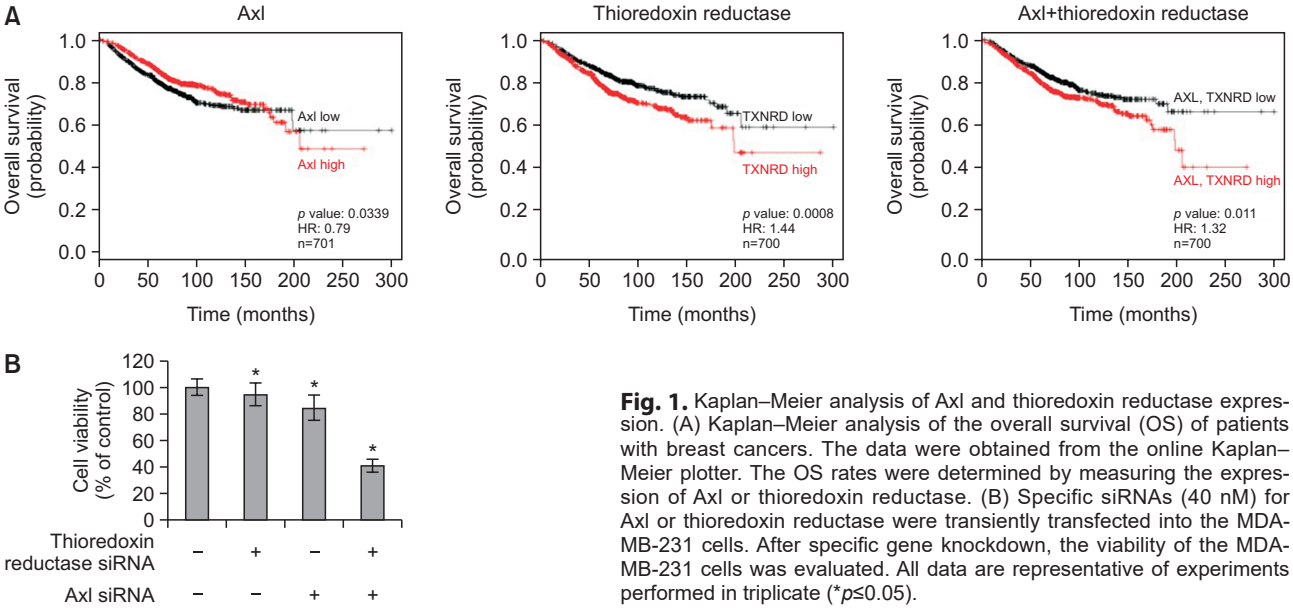

Fig. 1. Kaplan–Meier analysis of Axl and thioredoxin reductase expression. (A) Kaplan–Meier analysis of the overall survival (OS) of patients with breast cancers. The data were obtained from the online Kaplan–Meier plotter. The OS rates were determined by measuring the expression of Axl or thioredoxin reductase. (B) Specific siRNAs (40 nM) for Axl or thioredoxin reductase were transiently transfected into the MDA-MB-231 cells. After specific gene knockdown, the viability of the MDA-MB-231 cells was evaluated. All data are representative of experiments performed in triplicate (*$p \leq 0.05$).

Combination index (CI) values

The CI values were calculated using CompuSyn software (ComboSyn Inc., Paramus, NJ, USA) to examine the interactions between chemicals. The synergistic effects of the chemicals were evaluated via the isobologram method (Tallarida, 2001). Briefly, the IC_{50} value of each drug was plotted on the x- and y-axes to form a straight line. The data points in the isobologram correspond to the actual IC_{50} value of the combination of the chemicals. Data points on or near the line indicate an additive effect, those below the line indicate synergism, and those above the line represent antagonism.

Apoptosis assay

The cells were treated with the indicated concentrations of R428 and auranofin for 48 h, harvested with 0.05% trypsin-EDTA, and washed with PBS. The cells were then resuspended in PBS and stained with 0.2 mL of Muse™ Caspase 3/7 assay reagent (Millipore, CA, USA) for 30 min at room temperature in the dark. Apoptotic cells were detected using the Muse™ Cell Analyzer (Millipore) according to the manufacturer's instructions.

Wound healing assay

The cells (0.4×10^6 cells/well) were cultured in 12-well culture plates at 37°C in a humidified 5% CO_2 atmosphere. After 24 h, the cells at 90% confluency were washed with PBS and treated with mitomycin C (10 μg/mL) for 60 min. After washing several times, a single wound line was made per layer using a sterile 200-μL pipette tip. After removing the debris with PBS, the cells were incubated in RPMI 1640 medium containing the drugs. After the indicated durations of time, the cells that migrated into the wound area or protruded from the border of the wound were visualized and photographed under an inverted microscope.

Statistical analysis

Statistical analyses were performed using one-way analysis of variance, followed by Dunnett's multiple comparison test with GraphPad Prism 7 software (GraphPad Software Inc., San Diego, CA, USA). The differences were considered statistically significant at $p<0.05$.

RESULTS

Kaplan–Meier analysis of Axl or thioredoxin reductase expression

To determine the association between Axl or thioredoxin reductase expression and the overall survival (OS) of patients with different subtypes of breast cancer, Kaplan–Meier plots were generated using an online database (http://kmplot.com). Patients with high Axl or thioredoxin reductase expression showed lower OS rates than the control group, whereas patients with high expression of both genes showed the lowest OS rate (Fig. 1A). To confirm this result, the viability of breast cancer cells was assessed after gene knockdown using Axl kinase or thioredoxin reductase-specific siRNAs (40 nM). Treatment with Axl or thioredoxin reductase siRNAs significantly inhibited cell growth in the MDA-MB-231 cells (Fig. 1B).

Inhibition of breast cancer cell proliferation by single or combined treatment with R428 and auranofin

To determine whether R428 or auranofin exerted cytotoxic effects in human breast cancer cells, cell viability assays were performed in the MDA-MB-231 and MCF-7 cells. The results showed that treatment with R428 or auranofin alone inhibited the proliferation of cancer cells in a concentration-dependent manner. The IC_{50} values of R428 and auranofin were 11.63 ± 0.05 and 0.6 ± 0.03 μM, respectively (Fig. 2A, 2B), in the MDA-MB-231 cells and 7.86 ± 0.1 and 0.47 ± 0.02 μM, respectively (Fig. 2A, 2B), in the MCF-7 cells. These data showed that auranofin is a relatively stronger inhibitor of breast cancer cell proliferation.

To determine the effect of treatment with R428 and auranofin in combination, concentrations that maintained cell viability at approximately 80-85% were determined. The optimal

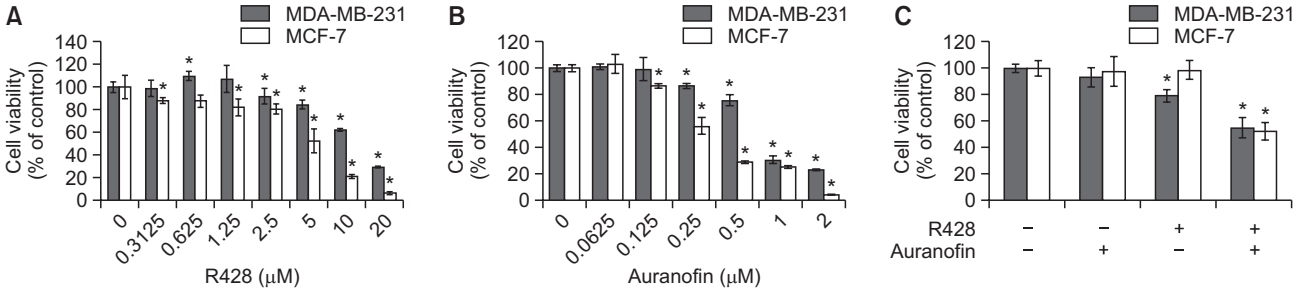

Fig. 2. The effect of R428 or auranofin treatment on breast cancer cells. (A) Inhibition of breast cancer cell proliferation by R428. The MDA-MB-231 and MCF-7 cells were treated with R428 (0, 0.3125, 0.625, 1.25, 2.5, 5, 10, or 20 μM) for 48 h. The CCK assay was performed to determine cell viability. Data are representative of experiments performed in triplicate (*$p \leq 0.05$). (B) Inhibition of breast cancer cell proliferation by auranofin. Cells were treated with auranofin (0, 0.0625, 0.125, 0.25, 0.5, 1, or 2 μM) for 48 h. The CCK assay was performed to determine cell viability. All data are representative of experiments performed in triplicate (*$p \leq 0.05$). (C) Cells were treated with a combination of R428 (2.5 μM) and auranofin (0.25 μM) for 48 h. The CCK assay was performed to determine cell viability. All data are representative of experiments performed in triplicate (*$p \leq 0.05$).

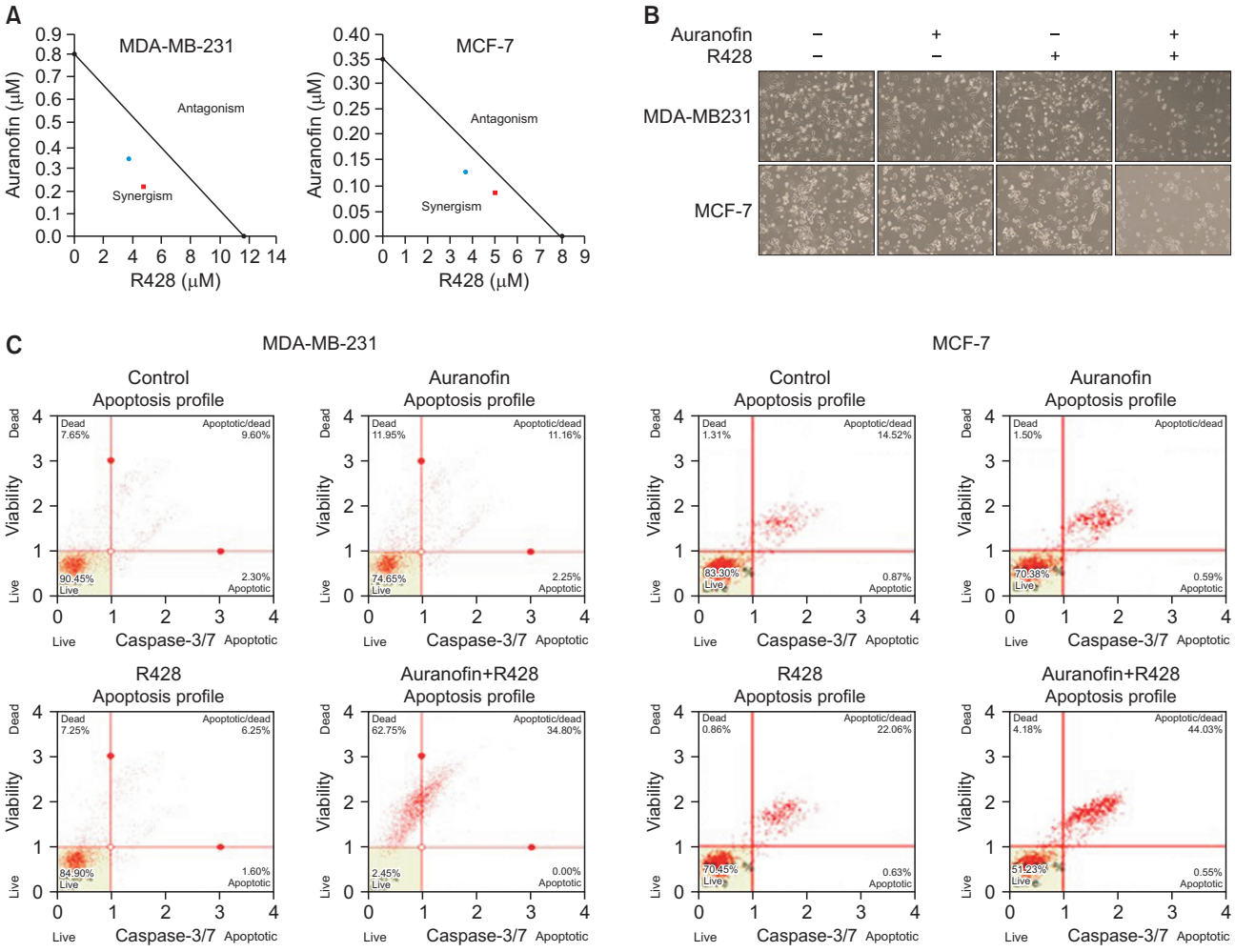

Fig. 3. Synergistic effects of R428 and auranofin in combination. (A) Isobologram analysis of the anti-proliferative effects of combination treatment with R428 (2.5 μM) and auranofin (0.25 μM) was performed and synergism was analyzed in the MDA-MB-231 and MCF-7 cells. (B) The morphology of the MDA-MB-231 and MCF-7 cells was observed by microscopy. Scale bar=20 μm. (C) Cell apoptosis was detected by flow cytometry. The cells were treated with Muse™ Caspase 3/7 reagent. After incubation for 30 min at 37°C, cell viability and density were measured using the Muse™ cell analyzer. All data are representative of experiments performed in triplicate.

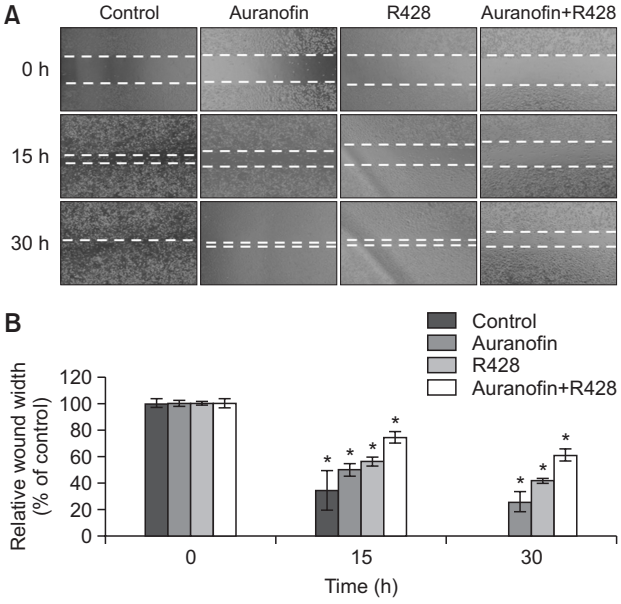

Fig. 4. Inhibition of cancer cell migration by combination treatment with R428 and auranofin. The MDA-MB-231 cells were treated with R428 (2.5 μM), auranofin (0.25 μM), or a combination of both for 48 h. (A) The wound area was measured at the indicated time points (0, 15, and 30 h) by microscopy. (B) Cell migration was assessed based on wound recovery. The relative wound width was calculated in three randomly selected microscopic fields. The data are presented as the means ± standard error of mean (n=3). *p<0.05 indicates a statistically significant difference compared to the control.

concentrations of R428 and auranofin were selected to be 2.5 and 0.25 μM, respectively. Combination treatment with R428 (2.5 μM) and auranofin (0.25 μM) resulted in a 56.2 ± 3.2% decrease in cell viability in the MDA-MB-231 cells and a 48.2 ± 5.6% decrease in the MCF-7 cells, indicating that the combination treatment was slightly more effective in the MCF-7 cells (Fig. 2C).

Synergistic effects of R428 and auranofin when used in combination

To determine whether R428 and auranofin showed synergistic effects when used in combination, the CI values were calculated from the IC_{50} values of the dose-response curve. The drugs in a drug-drug combination are considered to have synergistic effects if the CI value is less than 1. The CI values of the MDA-MB-231 cells treated with R428 (2.5 μM) and auranofin (0.125 or 0.25 μM) were 0.73 and 0.64, respectively (Fig. 3A, left). Because the CI value was less than 1, R428 and auranofin were considered to exert synergistic effects when used in combination in the MDA-MB-231 cells. Additionally, in the MCF-7 cells treated with R428 and auranofin, the CI values were found to be 0.73 and 0.85, respectively (Fig. 3A, right). Again, since the CI value was less than 1, R428 and auranofin were considered to exert synergistic effects when used in combination in the MCF-7 cells. Cell morphology was then observed under a microscope before harvesting 48 h after drug treatment. The results confirmed that the combination treatment strongly inhibited cell growth and proliferation (Fig. 3B). Furthermore, flow cytometry analysis revealed the strong induction of apoptosis upon combination treatment with R428 and auranofin in the MDA-MB-231 and MCF-7 cells (Fig. 3C).

Inhibition of cancer cell migration by combination treatment with R428 and auranofin

To investigate whether the combination of R428 and auranofin inhibited the migration of the MDA-MB-231 cells, the wound healing assay was performed. In the control cells, the wound was completely closed within 30 h after the scratch (Fig. 4A). However, compared to the control cells, wound closure (after 30 h) was inhibited by about 45% in the cancer cells. As shown in Fig. 4A, the relative wound width at 0, 15, or 30 h was plotted (Fig. 4B). These results suggest that R428 and auranofin may have synergistic effects on cell mobility or metastasis when used in combination in the MDA-MB-231 cells.

R428 and auranofin in combination synergistically induce apoptosis by increasing Bax and decreasing X-linked inhibitor of apoptosis protein (XIAP) expression

To investigate the mechanism by which the combination of R428 and auranofin inhibits the proliferation of human breast cancer cells, the levels of apoptosis-related proteins were measured. The results showed that combination treatment resulted in a higher level of Bax protein expression compared to single treatment in both the MDA-MB-231 and MCF-7 cells. When the combination of the two drugs was used, the expression of Bax was significantly increased, whereas that of XIAP was significantly decreased; however, the level of cleaved PARP was moderately increased (Fig. 5A). Moreover, the confocal microscopy results also revealed that Bax protein expression was significantly induced upon treatment with R428 and auranofin in combination (Fig. 5B).

Combination treatment with R428 and auranofin induces ROS generation and NAC inhibits this effect

To determine whether the synergistic effects of the two drugs in combination are related to ROS production, NAC was used to prevent ROS generation. When the cells were pretreated with NAC (5 mM), the combination treatment-induced reduction in cell viability was attenuated (Fig. 6A). Moreover, the increase in Bax protein expression induced by treatment with R428 and auranofin in combination was also suppressed by NAC treatment in the MDA-MB-231 cells (Fig. 6B). In addition, the combination treatment-induced decrease in XIAP expression was reversed and cleaved PARP levels were reduced by NAC treatment. The confocal microscopy results further confirmed that the increase in the Bax protein level induced by the combination treatment was attenuated by NAC in the MDA-MB-231 cells (Fig. 6C).

Combination treatment with R428 and auranofin induces cell death in liver, prostate, and breast cancer cells

Next, to determine whether the two drugs induced synergic effects on cancer cell apoptosis, cell viability was measured in Hep3B hepatocellular carcinoma, PC-3 prostate cancer, HeLa cervical cancer, and H520 non-small cell lung cancer cells. The results showed that the two drugs, when used in combination, had synergistic effects on apoptosis in the Hep3B and PC-3 cells (Fig. 7A, 7B). In contrast, the apoptotic effects were less significant in the lung and cervical cancer cells (Fig. 7C, 7D). Collectively, our data suggest that auranofin and R428

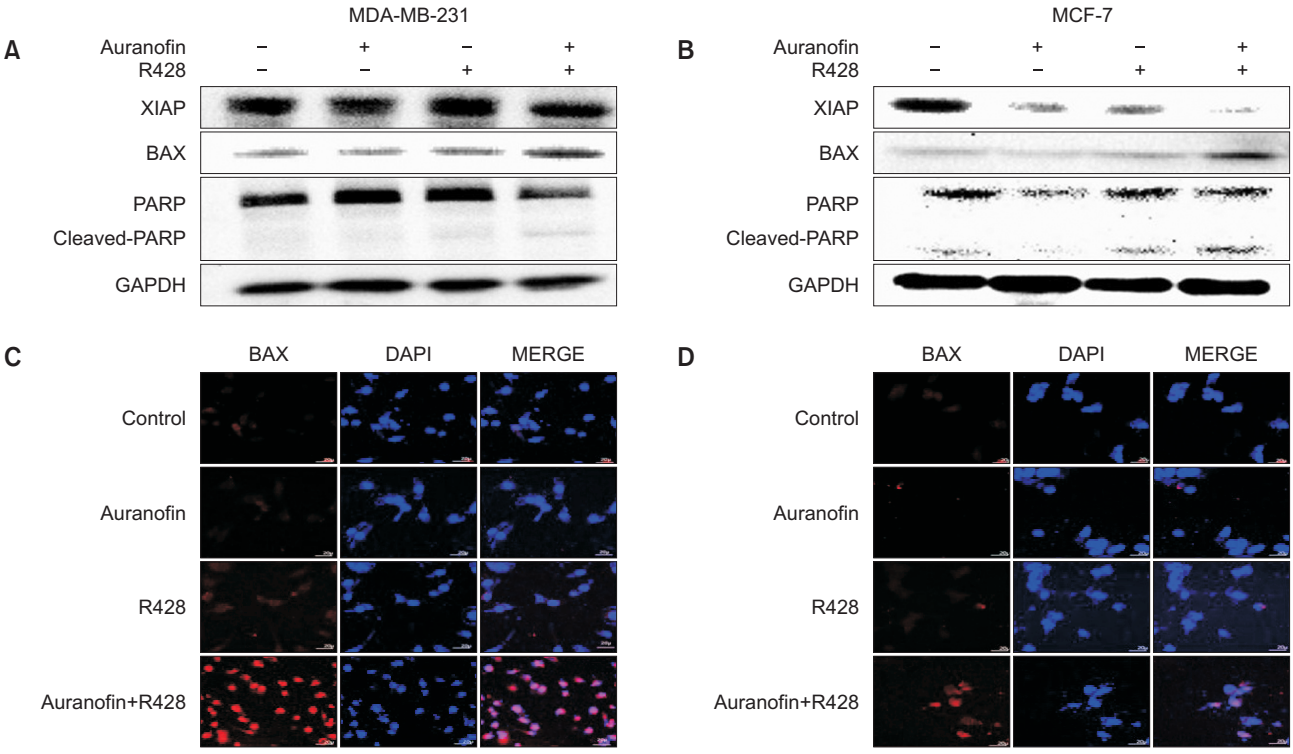

Fig. 5. R428 and auranofin in combination synergistically induce apoptosis by increasing Bax and decreasing XIAP expression. (A, B) The MDA-MB-231 and MCF-7 cells were co-treated with R428 (2.5 μM) and auranofin (0.25 μM) for 48 h. Western blot analysis was used to detect the proteins levels using XIAP, Bax, PARP, and GAPDH antibodies. GAPDH was used as the loading control. All data are representative of experiments performed in triplicate. (C, D) Confocal microscopy. The cells were plated on microscope slides and treated with the indicated drug concentrations. Bax expression was detected using the Bax antibody, followed by staining with the Texas Red-conjugated secondary antibody. DAPI was used for nuclear staining. Cells were then imaged under a confocal microscope. Scale bar=20 μm.

synergistically induced higher levels of apoptosis in the MCF-7, MDA-MB-231, PC-3, and Hep3B cells than in the HeLa and H520 cells.

DISCUSSION

Breast cancer can be classified according to the expression of membrane receptors, including ER, PR, and HER2. TNBC refers to any breast cancer that does not express ER, PR, and HER2. TNBC is more difficult to cure because no approved targeted therapies using monoclonal antibodies are currently available (Katz and Alsharedi, 2017). Therefore, chemotherapy is considered first-line treatment for patients with TNBC. Combination therapy with various anticancer agents can enhance treatment efficacy compared to single drug therapy because different carcinogenic pathways are targeted in synergistic or additive ways (Bayat Mokhtari *et al*., 2017).

Recently, auranofin was shown to promote cancer cell apoptosis to a greater extent than cisplatin in MCF-7 cells (Varghese and Busselberg, 2014). In our previous study, using an uPA inhibitor, we showed that auranofin exerted synergistic effects on apoptosis in breast cancer cells (Lee *et al*., 2017). Because R428, an Axl inhibitor, acts synergistically with cisplatin to inhibit hepatoma and prostate cancer metastases (Holland *et al*., 2010), we investigated the synergistic effects of R428 and auranofin in breast cancer cells. Our results confirmed that single treatment with R428 or auranofin reduced the viability of breast cancer cells in a concentration-dependent manner (Fig. 2A, 2B). Moreover, a synergistic apoptotic effect was observed when these drugs were combined at specific concentrations (Fig. 2C). In addition, the CI values showed a clear synergism between R428 and auranofin in both the MDA-MB-231 and MCF-7 cells (Fig. 3A).

Next, our findings revealed that combination treatment significantly increased Bax expression and decreased XIAP levels to promote apoptosis (Fig. 5A, 5B). Bax, a member of the pro-apoptotic Bcl-2 family of proteins, controls an important step in apoptosis by regulating mitochondrial outer membrane permeabilization (Shamas-Din *et al*., 2013). The association of Bax with the mitochondria is triggered by apoptotic signals. Bax forms a dimer, which, in turn, initiates permeation through the mitochondrial outer membrane (Maes *et al*., 2017). The insertion of Bax into the mitochondrial membrane induces cytochrome C release and increases apoptosis (Pawlowski and Kraft, 2000). Therefore, the increased permeability of the mitochondrial inner membrane caused by Bax induction may induce apoptosis. Here, we showed that co-treatment with R428 and auranofin increased apoptosis through Bax induction and XIAP downregulation in both the MCF-7 and MDA-MB-231 cells (Fig. 3C, 5A). Interestingly, Axl is known to inhibit Bax activity by Bcl-x_L induction through the NF-κB signaling pathway in various cancer cells (Lee *et al*., 2002; Tang *et al*., 2016). A previous study showed that auranofin inhibited NF-κB activa-

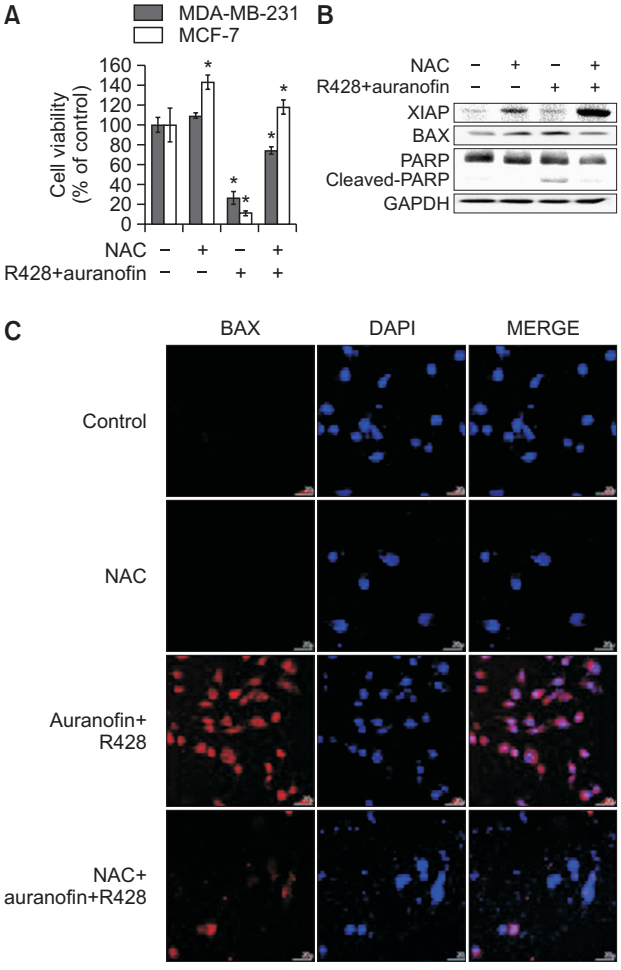

Fig. 6. The combination of R428 and auranofin induces ROS production and NAC recovers cell viability. (A) The MDA-MB-231 and MCF-7 cells were pre-treated with NAC (5 mM) for 2 h and then treated with R428 (2.5 μM) or auranofin (0.25 μM) for 48 h. Cell viability was measured via the CCK assay. Formazan formation was assessed by spectrophotometry at 450 nm. The ratio of the live cells in each group was calculated as a percentage of the control. All data are representative of experiments performed in triplicate (*p≤0.05). (B) Western blot analysis was used to detect the protein levels of XIAP, Bax, PARP, and GAPDH. GAPDH was used as the loading control. All data are representative of experiments performed in triplicate (*p≤0.05). (C) The alterations in Bax expression by NAC or the combination treatment were detected by confocal microscopy. Scale bar=20 μm.

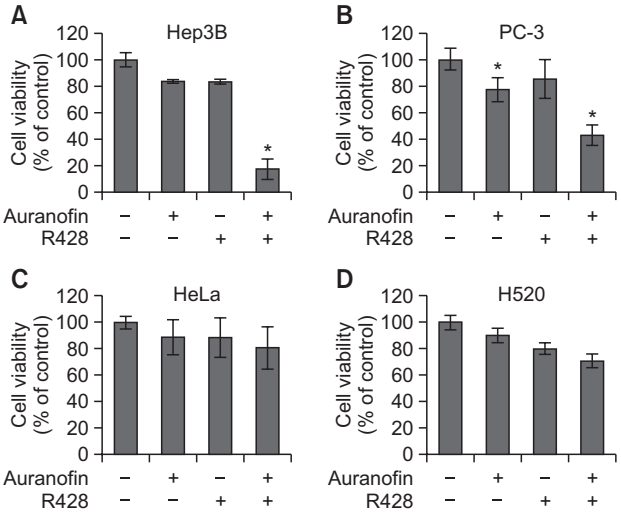

Fig. 7. Combination treatment with R428 and auranofin induces cell death in liver, prostate, and breast cancer cells. The (A) Hep3B, (B) PC-3, (C) HeLa, and (D) H520 cells were treated with a combination of R428 (2.5 μM) and auranofin (0.25 μM) for 48 h. Cell viability was measured via the CCK assay. Formazan formation was assessed by spectrophotometry at 450 nm. The ratio of the live cells in each group was calculated as a percentage of the control. All data are representative of experiments performed in triplicate (*p≤0.05).

tion by blocking IκB kinase activity, subsequently promoting apoptosis in cancer cells (Cuadrado *et al*., 2014). Hence, the combination of R428 and auranofin may induce cancer cell apoptosis through Bax activation by inhibiting NF-κB signaling.

NAC, an inhibitor of ROS generation, has been widely used as an antioxidant to investigate the role of ROS in the induction of apoptosis (Sun, 2010). If Bax was increased through ROS generation and promotes cell apoptosis, the increased Bax level and inhibition of cell viability would be recovered when NAC was added to the R428 and auranofin co-treated cells. Here, we found that the combination treatment-induced reduction in cell viability and increase in Bax expression were reversed to the control levels by NAC treatment (Fig. 6).

Interestingly, as shown in Fig. 7, the synergistic induction of cell death was observed in the Hep3B and PC-3 cells, but the combination treatment had no synergistic effects on the HeLa and H520 cells. Under normal cell conditions, ROS generation is maintained at a low level (Kapur *et al*., 2018). Excessive ROS production induces oxidative stress, including apoptosis. Nuclear factor erythroid 2-related factor 2 (NRF2)/Kelch-like ECH-associated protein 1 (KEAP1) signaling is one of the pivotal defense systems against oxidative stress in cancer cells. The excessive generation of ROS promotes the degradation of the KEAP1 protein, inducing NRF2 nuclear translocation. Nuclear NRF2 is known to increase the level of antioxidant genes such as Gpx2 and Gstp1 (Lu *et al*., 2017; Cuadrado *et al*., 2018; Chu *et al*., 2020). Cells that show clear synergistic cell death upon treatment with auranofin and R428, such as the MDA-MB-231, MCF-7, PC-3, and Hep3B cells, are known to have low levels of NRF2 activity. In contrast, the HeLa and H520 cells have relatively higher NRF2 activity (Zhang *et al*., 2010; Cazanave *et al*., 2014; Mine *et al*., 2014; Lu *et al*., 2017; Richa *et al*., 2020). Since the synergistic effect of auranofin and R428 is expected to enhance ROS production, it is presumed that the effect of the combination treatment might be weak in the NRF2-activated cancer cells. Interestingly, we found that the synergistic effect of auranofin and R428 is higher in the MDA-MB-231 cells than in the MCF-7 cells (Fig. 3A). A previous study also showed that the MDA-MB-231 cells have lower NRF2 activity than the MCF-7 cells (Probst *et al*., 2015).

Previous studies demonstrated that Axl inhibition suppresses breast cancer cell migration (Koorstra *et al*., 2009; Holland *et al*., 2010). Axl activation is known to promote cancer cell migration through Rac1 induction (Katoh *et al*., 2006; Faix

and Weber, 2013). Furthermore, auranofin has been shown to suppress Rac1 expression in cancer cells with impaired NRF2 activity (Cuadrado *et al*., 2014). While the exact mechanism of Rac1 is not yet clear, we speculate that the combination of R428 and auranofin might suppress cell migration through the inhibition of Rac1 expression.

Furthermore, we suggest that the effect of combination therapy might be affected by cellular antioxidative systems, including KEAP1/NRF2 signaling. Hence, the antioxidative systems in cancer cells might be the expected target of combined anticancer agents. In our study, we demonstrated the therapeutic significance of the novel combination of R428 and auranofin. Our findings suggest that R428 and auranofin might serve as good candidates for the combination therapy in breast cancer, especially TNBC, through the induction of apoptosis by ROS and the suppression of cancer cell migration.

CONFLICT OF INTEREST

The authors declare that they have no conflicts of interest.

ACKNOWLEDGMENTS

This research was supported by the National Research Foundation of Korea (NRF), funded by the Korean government (MSIP) (grant nos. NRF2017R1E1A1A01074032 and NRF2015R1A5A1008958). The funders had no role in the study design, data collection and analysis, the decision to publish, or manuscript preparation.

REFERENCES

Bayat Mokhtari, R., Homayouni, T. S., Baluch, N., Morgatskaya, E., Kumar, S., Das, B. and Yeger, H. (2017) Combination therapy in combating cancer. *Oncotarget* **8**, 38022-38043.

Cazanave, S. C., Wang, X., Zhou, H., Rahmani, M., Grant, S., Durrant, D. E., Klaassen, C. D., Yamamoto, M. and Sanyal, A. J. (2014) Degradation of Keap1 activates BH3-only proteins Bim and PUMA during hepatocyte lipoapoptosis. *Cell Death Differ.* **21**, 1303-1312.

Chu, C., Gao, X., Li, X., Zhang, X., Ma, R., Jia, Y., Li, D., Wang, D. and Xu, F. (2020) Involvement of estrogen receptor-α in the activation of Nrf2-antioxidative signaling pathways by silibinin in pancreatic β-cells. *Biomol. Ther. (Seoul)* **28**, 163-171.

Cuadrado, A., Manda, G., Hassan, A., Alcaraz, M. J., Barbas, C., Daiber, A., Ghezzi, P., Leon, R., Lopez, M. G., Oliva, B., Pajares, M., Rojo, A. I., Robledinos-Anton, N., Valverde, A. M., Guney, E. and Schmidt, H. (2018) Transcription factor NRF2 as a therapeutic target for chronic diseases: a systems medicine approach. *Pharmacol. Rev.* **70**, 348-383.

Cuadrado, A., Martin-Moldes, Z., Ye, J. and Lastres-Becker, I. (2014) Transcription factors NRF2 and NF-κB are coordinated effectors of the Rho family, GTP-binding protein RAC1 during inflammation. *J. Biol. Chem.* **289**, 15244-15258.

Faix, J. and Weber, I. (2013) A dual role model for active Rac1 in cell migration. *Small GTPases* **4**, 110-115.

Fiskus, W., Saba, N., Shen, M., Ghias, M., Liu, J., Gupta, S. D., Chauhan, L., Rao, R., Gunewardena, S., Schorno, K., Austin, C. P., Maddocks, K., Byrd, J., Melnick, A., Huang, P., Wiestner, A. and Bhalla, K. N. (2014) Auranofin induces lethal oxidative and endoplasmic reticulum stress and exerts potent preclinical activity against chronic lymphocytic leukemia. *Cancer Res.* **74**, 2520-2532.

Gay, C. M., Balaji, K. and Byers, L. A. (2017) Giving AXL the axe: targeting AXL in human malignancy. *Br. J. Cancer* **116**, 415-423.

Gelmon, K., Dent, R., Mackey, J. R., Laing, K., McLeod, D. and Verma, S. (2012) Targeting triple-negative breast cancer: optimising therapeutic outcomes. *Ann. Oncol.* **23**, 2223-2234.

Goyette, M. A., Duhamel, S., Aubert, L., Pelletier, A., Savage, P., Thibault, M. P., Johnson, R. M., Carmeliet, P., Basik, M., Gaboury, L., Muller, W. J., Park, M., Roux, P. P., Gratton, J. P. and Cote, J. F. (2018) The receptor tyrosine kinase Axl is required at multiple steps of the metastatic cascade during HER2-positive breast cancer progression. *Cell Rep.* **23**, 1476-1490.

Holland, S. J., Pan, A., Franci, C., Hu, Y., Chang, B., Li, W., Duan, M., Torneros, A., Yu, J., Heckrodt, T. J., Zhang, J., Ding, P., Apatira, A., Chua, J., Brandt, R., Pine, P., Goff, D., Singh, R., Payan, D. G. and Hitoshi, Y. (2010) R428, a selective small molecule inhibitor of Axl kinase, blocks tumor spread and prolongs survival in models of metastatic breast cancer. *Cancer Res.* **70**, 1544-1554.

Jin, S. and Ye, K. (2013) Targeted drug delivery for breast cancer treatment. *Recent Pat. Anticancer Drug Discov.* **8**, 143-153.

Jung, J. (2019) Role of G protein-coupled estrogen receptor in cancer progression. *Toxicol. Res.* **35**, 209-214.

Kapur, A., Beres, T., Rathi, K., Nayak, A. P., Czarnecki, A., Felder, M., Gillette, A., Ericksen, S. S., Sampene, E., Skala, M. C., Barroilhet, L. and Patankar, M. S. (2018) Oxidative stress via inhibition of the mitochondrial electron transport and Nrf-2-mediated anti-oxidative response regulate the cytotoxic activity of plumbagin. *Sci. Rep.* **8**, 1073.

Katoh, H., Hiramoto, K. and Negishi, M. (2006) Activation of Rac1 by RhoG regulates cell migration. *J. Cell Sci.* **119**, 56-65.

Katz, H. and Alsharedi, M. (2017) Immunotherapy in triple-negative breast cancer. *Med. Oncol.* **35**, 13.

Koorstra, J. B., Karikari, C. A., Feldmann, G., Bisht, S., Rojas, P. L., Offerhaus, G. J., Alvarez, H. and Maitra, A. (2009) The Axl receptor tyrosine kinase confers an adverse prognostic influence in pancreatic cancer and represents a new therapeutic target. *Cancer Biol. Ther.* **8**, 618-626.

Leconet, W., Chentouf, M., du Manoir, S., Chevalier, C., Sirvent, A., Ait-Arsa, I., Busson, M., Jarlier, M., Radosevic-Robin, N., Theillet, C., Chalbos, D., Pasquet, J. M., Pelegrin, A., Larbouret, C. and Robert, B. (2017) Therapeutic activity of anti-Axl antibody against triple-negative breast cancer patient-derived xenografts and metastasis. *Clin. Cancer Res.* **23**, 2806-2816.

Lee, J. E., Kwon, Y. J., Baek, H. S., Ye, D. J., Cho, E., Choi, H. K., Oh, K. S. and Chun, Y. J. (2017) Synergistic induction of apoptosis by combination treatment with mesupron and auranofin in human breast cancer cells. *Arch. Pharm. Res.* **40**, 746-759.

Lee, W. P., Wen, Y., Varnum, B. and Hung, M. C. (2002) Akt is required for Axl-Gas6 signaling to protect cells from E1A-mediated apoptosis. *Oncogene* **21**, 329-336.

Lu, K., Alcivar, A. L., Ma, J., Foo, T. K., Zywea, S., Mahdi, A., Huo, Y., Kensler, T. W., Gatza, M. L. and Xia, B. (2017) NRF2 induction supporting breast cancer cell survival is enabled by oxidative stress-induced DPP3-Keap1 interaction. *Cancer Res.* **77**, 2881-2892.

Maes, M. E., Schlamp, C. L. and Nickells, R. W. (2017) Live-cell imaging to measure Bax recruitment kinetics to mitochondria during apoptosis. *PLoS ONE* **12**, e0184434.

Miller, M. A., Oudin, M. J., Sullivan, R. J., Wang, S. J., Meyer, A. S., Im, H., Frederick, D. T., Tadros, J., Griffith, L. G., Lee, H., Weissleder, R., Flaherty, K. T., Gertler, F. B. and Lauffenburger, D. A. (2016) Reduced proteolytic shedding of receptor tyrosine kinases is a post-translational mechanism of kinase inhibitor resistance. *Cancer Discov.* **6**, 382-399.

Mine, N., Yamamoto, S., Kufe, D. W., Von Hoff, D. D. and Kawabe, T. (2014) Activation of Nrf2 pathways correlates with resistance of NSCLC cell lines to CBP501 *in vitro*. *Mol. Cancer Ther.* **13**, 2215-2225.

Nagini, S. (2017) Breast cancer: current molecular therapeutic targets and new players. *Anticancer Agents Med. Chem.* **17**, 152-163.

Oommen, D., Yiannakis, D. and Jha, A. N. (2016) BRCA1 deficiency increases the sensitivity of ovarian cancer cells to auranofin. *Mutat. Res.* **784-785**, 8-15.

Pawlowski, J. and Kraft, A. S. (2000) Bax-induced apoptotic cell death. *Proc. Natl. Acad. Sci. U.S.A.* **97**, 529-531.

Probst, B. L., McCauley, L., Trevino, I., Wigley, W. C. and Ferguson,

D. A. (2015) Cancer cell growth is differentially affected by constitutive activation of NRF2 by Keap1 deletion and pharmacological activation of NRF2 by the synthetic triterpenoid, RTA 405. *PLoS ONE* **10**, e0135257.

Richa, S., Dey, P., Park, C., Yang, J., Son, J. Y., Park, J. H., Lee, S. H., Ahn, M. Y., Kim, I. S., Moon, H. R. and Kim, H. S. (2020) A new histone deacetylase inhibitor, MHY4381, induces apoptosis via generation of reactive oxygen species in human prostate cancer cells. *Biomol. Ther. (Seoul)* **28**, 184-194.

Shamas-Din, A., Kale, J., Leber, B. and Andrews, D. W. (2013) Mechanisms of action of Bcl-2 family proteins. *Cold Spring Harb. Perspect. Biol.* **5**, a008714.

Shaw, I. C. (1999) Gold-based therapeutic agents. *Chem. Rev.* **99**, 2589-2600.

Sun, S. Y. (2010) N-acetylcysteine, reactive oxygen species and beyond. *Cancer Biol. Ther.* **9**, 109-110.

Tallarida, R. J. (2001) Drug synergism: its detection and applications. *J. Pharmacol. Exp. Ther.* **298**, 865-872.

Tang, B., Tang, F., Wang, Z., Qi, G., Liang, X., Li, B., Yuan, S., Liu, J., Yu, S. and He, S. (2016) Upregulation of Akt/NF-κB-regulated inflammation and Akt/Bad-related apoptosis signaling pathway involved in hepatic carcinoma process: suppression by carnosic acid nanoparticle. *Int. J. Nanomedicine* **11**, 6401-6420.

Varghese, E. and Busselberg, D. (2014) Auranofin, an anti-rheumatic gold compound, modulates apoptosis by elevating the intracellular calcium concentration in MCF-7 breast cancer cells. *Cancers (Basal)* **6**, 2243-2258.

Vidula, N. and Bardia, A. (2017) Targeted therapy for metastatic triple negative breast cancer: the next frontier in precision oncology. *Oncotarget* **8**, 106167-106168.

Wang, C., Jin, H., Wang, N., Fan, S., Wang, Y., Zhang, Y., Wei, L., Tao, X., Gu, D., Zhao, F., Fang, J., Yao, M. and Qin, W. (2016) Gas6/Axl axis contributes to chemoresistance and metastasis in breast cancer through kat/GSK-3β/β-catenin signaling. *Theranostics* **6**, 1205-1219.

Yao, H., He, G., Yan, S., Chen, C., Song, L., Rosol, T. J. and Deng, X. (2017) Triple-negative breast cancer: is there a treatment on the horizon. *Oncotarget* **8**, 1913-1924.

Zhang, P., Singh, A., Yegnasubramanian, S., Esopi, D., Kombairaju, P., Bodas, M., Wu, H., Bova, S. G. and Biswal, S. (2010) Loss of Kelch-like ECH-associated protein 1 function in prostate cancer cells causes chemoresistance and radioresistance and promotes tumor growth. *Mol. Cancer Ther.* **9**, 336-346.

Zhang, Y. X., Knyazev, P. G., Cheburkin, Y. V., Sharma, K., Knyazev, Y. P., Orfi, L., Szabadkai, I., Daub, H., Keri, G. and Ullrich, A. (2008) Axl is a potential target for therapeutic intervention in breast cancer progression. *Cancer Res.* **68**, 1905-1915.